

REMARKS ON POWER-LAW RANDOM GRAPHS

MEI YIN

We interpret a classical problem for the Poisson approximations for U -statistics in the context of random graphs. Our model is closely connected to a motivating example in Borgs et al. [Trans. Amer. Math. Soc. 372 (2019), 3019-3062], and may be termed a *power-law random graph without Bernoulli edges*. We examine the distinctively different structures of the limit graph in detail in all regimes, critical, super-critical, and sub-critical. Many interesting results are established. Though elementary at first sight, our model serves as an uncovered boundary case between different types of graph convergence.

Keywords Power-law random graph · Graph limit · Critical, super-critical, and sub-critical regimes

Mathematics Subject Classification 05C80 · 82B26

CONTENTS

1. A classical problem on U-statistics	1
1.1. A random-graph interpretation	2
2. A toy example	2
2.1. Critical regime: Classical results	3
2.2. Other regimes: First estimates	4
3. Super-critical regime	8
4. Sub-critical regime	10
5. On modes of graph convergence	15
6. Further discussions: Power-law random graph with Bernoulli edges	16
Acknowledgements	18
References	18

1. A CLASSICAL PROBLEM ON U-STATISTICS

Consider a collection of i.i.d. random variables $\{X_n\}_{n \in \mathbb{N}}$, and the following (max) U -statistics

$$Y_n := \max_{1 \leq i < j \leq n} h(X_i, X_j) \tag{1.1}$$

for some measurable symmetric function $h : \mathbb{R}^2 \rightarrow \mathbb{R}$. Such a framework has been considered implicitly in [7]. Indeed, rather than optimization, summation was considered therein, but since $h(X_i, X_j)$ was assumed to have a regularly-varying tail, the sum- and max-problems do not differ much. Essentially both are based on the point-process convergence of

$$\sum_{1 \leq i < j \leq n} \delta_{(h(X_i, X_j)/a_n, i/n, j/n)} \tag{1.2}$$

for some appropriate a_n . This convergence is powerful in that it captures all information of the underlying dynamics; the limit of (1.2) for example entails the limit of Y_n/a_n , among many other things.

However, a key assumption in [7] limits significantly the potential range of applications. This so-called *anti-clustering* condition assures that asymptotically the limit of (1.2) is a Poisson point process. See [7, Equation 2.1]. We provide here a brief explanation. Consider $h(X_i, X_j)$ alone first. Clearly, for a non-trivial convergence of (1.2), necessarily we would need the average number of points $h(X_i, X_j)$ exceeding x after

a_n -scaling to be of order $O(1)$:

$$\sum_{1 \leq i < j \leq n} \mathbb{P}(h(X_i, X_j) > a_n x) \sim C, \quad (1.3)$$

or equivalently

$$\mathbb{P}(h(X_i, X_j) > a_n x) \sim \frac{C}{n^2}. \quad (1.4)$$

For notational convenience, here and below, the constant C may change from line to line. If the limit is indeed Poisson, then the two-moment-suffices principle [1] applies. The condition on second moments becomes

$$\sum_{1 \leq i < j \leq n} \sum_{\substack{(i,j) \neq (i',j') \in [n]^2 \\ i'=i \text{ or } j'=j}} \mathbb{P}(h(X_i, X_j) > a_n x, h(X_{i'}, X_{j'}) > a_n x) = o(1), \quad (1.5)$$

or equivalently

$$\mathbb{P}(h(X_i, X_j) > a_n x, h(X_{i'}, X_{j'}) > a_n x) = o(n^{-3}). \quad (1.6)$$

We refer to (1.6) as an anti-clustering condition, as it says that heuristically very large values of $h(X_1, X_2)$ and $h(X_1, X_3)$ occur separately from each other, among others. More precisely, if $\mathbb{P}(h(X_1, X_2) > x) \sim x^{-\beta}$ for some $\beta > 0$ and (1.6) holds, then the limit of (1.2) is $\text{PPP}(Cx^{-\beta} dx dudv)$ on $(0, \infty] \times [0, 1] \times [0, 1]$. Nevertheless, note the difference between the setup in [7] and the present setup: They consider small values near zero, while we consider large values near infinity.

1.1. A random-graph interpretation. Fix a threshold x_0 throughout. Then, if $h(X_i, X_j) > a_n x_0$, we set the adjacency matrix, $A_n = (a_{n,i,j})_{1 \leq i, j \leq n}$, to have entry $a_{n,i,j} = 1$ and otherwise 0. If we further drop all the isolated vertices (those with no incident edges), then we end up with a random graph which is obviously exchangeable. Is there anything one can say explicitly about the limit of this random graph?

Under the current framework, in addition to (1.4), the anti-clustering condition (1.6) holds, which basically states that if there is an edge placed between i and j , then the conditional probability that either i or j is connected to any other vertex goes to zero. In other words, all edges in the limit are not connected (no vertices have degree ≥ 2). This corresponds to the point-process limit of (1.2), with each point representing an isolated edge. In terms of sparse exchangeable random graphs [2, 6, 8, 9], the graph limit has only *dust* part, which has nothing but trivial structure. But what happens to the graph limit when the anti-clustering condition (1.6) is violated while (1.4) is still kept? Will the limiting graph display a non-trivial structure?

These questions and more will be addressed in the following sections. We start with explicit calculations for a basic random graph model in Section 2 and then generalize the model further in Section 4. We will examine the distinctively different structures of the limit graph in detail in all regimes, critical, super-critical, and sub-critical. As Section 5 illustrates, our model is closely connected to a motivating example in [4]. Though elementary at first sight, it serves as an uncovered boundary case between different types of graph convergence.

We list some highlights of our investigation.

- (i) At the super-critical regime, in the rare event that we do see a non-empty graph, typically it has exactly two vertices, one clique vertex and one follower vertex.
- (ii) At the super-critical regime, when Bernoulli edges are taken into consideration as in [4], some abrupt changes occur in the quality of the limiting object.
- (iii) At the sub-critical regime, our model displays an interesting *anti-transitive* characteristic concerning the appearance of triangles vs. two-stars.
- (iv) At the sub-critical regime, we observe universality in the graph limit. After proper scaling, the parameter influence on the relation between number of vertices/edges disappears asymptotically.

2. A TOY EXAMPLE

For a prototype model, for $\alpha > 0$, consider

$$h(x, y) = xy \quad \text{with} \quad \mathbb{P}(X_i > x) \sim x^{-\alpha}, \quad (2.1)$$

then condition (1.6) fails by a large margin. Here one could actually take the i.i.d. X_i to have pdf $\alpha x^{-\alpha-1} dx \mathbf{1}_{\{x \geq 1\}}$ to make all calculations explicit, and yet have the same asymptotic phenomenon.

2.1. Critical regime: Classical results. The first obvious normalization that produces a non-degenerate graph limit is easily seen. It is well known that

$$\sum_{i=1}^n \delta_{(X_i/n^{1/\alpha}, i/n)} \text{ converges weakly to } \sum_{i=1}^{\infty} \delta_{(\Gamma_i^{-1/\alpha}, U_i)}, \quad (2.2)$$

where the parameter $\alpha > 0$, $\{\Gamma_n\}_{n \in \mathbb{N}}$ is the consecutive arrival times of a standard Poisson process and $\{U_n\}_{n \in \mathbb{N}}$ are i.i.d. $(0, 1)$ -uniform random variables, the two series being independent. From this observation, a suitable representation for the limiting random graph may be identified. Let

$$W(x, y) := \mathbf{1}_{\{xy > x_0\}}, \quad x, y > 0. \quad (2.3)$$

View W as a graphon on the measure space $((0, \infty), \mathcal{B}((0, \infty)), \alpha x^{-\alpha-1} dx \mathbf{1}_{\{x \geq 1\}})$, and take $I = S = 0$ in the graphex process representation. The corresponding graphex process can then be defined as follows. Let $\sum_{i=1}^{\infty} \delta_{(\theta_i, U_i)}$ be a PPP on $(0, \infty) \times (0, \infty)$ with intensity measure $\alpha x^{-\alpha-1} dx \mathbf{1}_{\{x \geq 1\}} \otimes du$. For each $t > 0$, we construct the graph \mathcal{G}_t iteratively:

- (i) Consider all vertices i such that $U_i \leq t$, denoted by $\tilde{V}_t := \{i : U_i \leq t\}$.
- (ii) Connect $i \sim j$ with $i, j \in \tilde{V}_t$ with a Bernoulli random variable with parameter $W(\theta_i, \theta_j)$, conditionally independent from all other edges given the PPP.
- (iii) Keep only those vertices $i \in \tilde{V}_t$ with degrees strictly positive, denoted by V_t , and edges between them, denoted by E_t . (This last step is not essential.)

Obviously, the process $\{\mathcal{G}_t\}_{t \geq 0}$ is nested if the labels of vertices are ignored.

Proposition 2.1. The empirical random graph in the toy model at the critical regime ($a_n \sim n^{2/\alpha}$) converges in distribution to the random graph \mathcal{G}_1 .

Proof. We recognize that this statement is merely a fancy interpretation of the well-known fact (2.2). Convergence of the underlying point process (1.2) ensures convergence of the *random adjacency measures*. In this convergence, the choice of W as in (2.3) is not unique. \square

The below alternate representation for \mathcal{G}_t will present a more explicit construction. Set

$$\mathcal{N}_t := \{(\theta_i, U_i)\}_{U_i \leq t}. \quad (2.4)$$

We first ask how many points $(\theta, U) \in \mathcal{N}_t$ are such that $\theta > \sqrt{x_0}$ and $U \leq t$. This is a Poisson number, denoted by $K_0 = K_{t, x_0}$, with parameter

$$\int_{\sqrt{x_0}}^{\infty} \int_0^t \alpha x^{-\alpha-1} du d\theta = t x_0^{-\alpha/2}. \quad (2.5)$$

If $K_0 = 0$ then there is no graph. So suppose $K_0 > 0$ from now on, and let $\{\tilde{\theta}_j, \tilde{U}_j\}_{j=1, \dots, K_0}$ be the collection of all such points in the order $\tilde{\theta}_1 \geq \tilde{\theta}_2 \geq \dots \geq \tilde{\theta}_{K_0} > \sqrt{x_0}$. Next we examine all the remaining points (θ, U) (so that they are not among the K_0 ones above). If $\theta < x_0/\tilde{\theta}_1$, it does not contribute to the random graph, so it suffices to focus on $\theta \in (x_0/\tilde{\theta}_1, \sqrt{x_0})$. We further divide this interval into

$$\left(\left(\frac{x_0}{\tilde{\theta}_{K_0}}, \sqrt{x_0} \right], \left(\frac{x_0}{\tilde{\theta}_{K_0-1}}, \frac{x_0}{\tilde{\theta}_{K_0}} \right], \dots, \left(\frac{x_0}{\tilde{\theta}_1}, \frac{x_0}{\tilde{\theta}_2} \right) \right) =: (I_1, \dots, I_{K_0}). \quad (2.6)$$

Conditioning on $K_0 > 0$ and $\{\tilde{\theta}_j, \tilde{U}_j\}_{j=1, \dots, K_0}$, the remaining points in \mathcal{N}_t again form a PPP on $(0, \sqrt{x_0}) \times (0, t)$ with intensity measure $\alpha x^{-\alpha-1} dx \mathbf{1}_{\{x \geq 1\}} \otimes du$. In particular the number of points in each of the intervals I_j above, denoted by K_1, \dots, K_{K_0} , are conditionally independent Poisson random variables, the parameters of which are computable (the θ -values of points in each interval do not play a role in the random graph eventually). Now, with K_0, \dots, K_{K_0} , the random graph \mathcal{G}_t can be constructed as follows.

- (i) The graph has a ‘clique’ with K_0 vertices, labeled by $1, \dots, K_0$.
- (ii) For each $j = 1, \dots, K_0$, add in addition K_j vertices that each connects to vertices indexed by $1, 2, \dots, K_0 + 1 - j$ (but not those by $K_0 + 2 - j, \dots, K_0$ for $j \geq 2$ nor all the other existed vertices).

Note that taking the corresponding time random variables U into account, one could actually recover $\{\mathcal{G}_s\}_{0 \leq s \leq t}$ in an obviously manner.

Remark 2.2. We refer to the vertices in the second step above as ‘followers’, as opposed to the ‘clique’ vertices in the first step. This construction itself is nothing special. It is more interesting to look at the analogous constructions for the discrete model, where there are counterparts for the ‘clique’ and ‘followers’, and it is of crucial importance to know how fast each part grows. We will come back to these notions at the end of Section 2.

2.2. Other regimes: First estimates. However, the normalization $a_n \sim n^{2/\alpha}$ established in Proposition 2.1 is not what is suggested by the Poisson approximation (1.4), which would require $a_n \sim n^{2/\alpha} \log n$. Indeed, with (2.1) we have

$$\mathbb{P}(X_1 X_2 > x) \sim \alpha x^{-\alpha} \log x. \quad (2.7)$$

(See [10, Lemma 4.1] for a summary on tails of product of random variables with power-law tails.) At the same time though, (1.6) fails, as in this case,

$$\mathbb{P}(X_1 X_2 > x, X_1 X_3 > x) \sim C x^{-\alpha}. \quad (2.8)$$

We still have the desired asymptotic tail-independence for $X_1 X_2$ and $X_1 X_3$, $\mathbb{P}(X_1 X_3 > x \mid X_1 X_2 > x) = C/\log x \rightarrow 0$ as $x \rightarrow \infty$, but this $\log x$ decay is too slow compared to what is needed for (1.6). Of course, for normalizations of different order from $n^{2/\alpha}$, we will not have any non-degenerate extreme-value limit as in Section 2.1. Nonetheless, it is interesting to inquire if a graph limit exists in certain sense.

Since the largest value among X_i goes to zero at the modified normalization $n^{2/\alpha} \log n$, there is no graph in the limit. This, and the fact that the average number of edges is a constant > 0 , show that the conditional number of edges of the graph given there is a non-empty graph is going to infinity. Generalizing further, if $a_n^\alpha \sim n^\gamma \log n$, then the average number of edges grows at the order of

$$\mathbb{E}|E_n| = \binom{n}{2} \cdot \alpha a_n^{-\alpha} \log(a_n) \sim \frac{\gamma}{2} n^{2-\gamma}. \quad (2.9)$$

There are two parameters α and γ that we could play with here. Will a non-trivial graph limit exist under some specified parameter ranges? We recognize that $X_i \stackrel{d}{=} U_i^{-1/\alpha}$ where U_i are i.i.d. $(0, 1)$ -uniform, which implies that

$$\left\{ \frac{X_i X_j}{a_n} > 1 \right\} = \left\{ U_i U_j < \frac{1}{n^\gamma \log n} \right\}, \quad (2.10)$$

so α is actually irrelevant as a parameter, and we can concentrate on fine tuning γ solely. In addition to the critical regime ($\gamma = 2$), following standard terminology, we refer to $\gamma < 2$ as the sub-critical regime and $\gamma > 2$ as the super-critical regime. The influence of $\log n$ will also be asymptotically insignificant against n^γ , as we will see in further investigations.

We explore these directions step by step, beginning with straightforward estimates to generate some first ideas. Other than the expected number of edges that was given above, one could compute many quantities for this toy model explicitly, for example the expected number of non-isolated vertices.

$$\mathbb{E}|V_n| \sim \begin{cases} 0 & \gamma > 2, \\ (\gamma - 1)n^{2-\gamma} & \gamma \in (1, 2], \\ n \frac{\log \log n}{\log n} & \gamma = 1, \\ n & \gamma \in (0, 1). \end{cases} \quad (2.11)$$

To see this, take X_i to have explicit pdf $\alpha x^{-\alpha-1} dx \mathbf{1}_{\{x \geq 1\}}$. Then for any $z > 1$,

$$\begin{aligned} \mathbb{P}\left(\max_{i=1, \dots, n-1} X_1 X_{1+i} > z\right) &= \int_1^\infty \alpha x^{-\alpha-1} dx \left[1 - \mathbb{P}\left(X_1 \leq \frac{z}{x}\right)^{n-1}\right] \\ &= \frac{1}{z^\alpha} + \int_1^z \alpha x^{-\alpha-1} dx \left[1 - \left(1 - \left(\frac{x}{z}\right)^\alpha\right)^{n-1}\right] \\ &= \frac{1}{z^\alpha} + \frac{n}{z^\alpha} \int_{n/z^\alpha}^n y^{-2} \left[1 - \left(1 - \frac{y}{n}\right)^{n-1}\right] dy. \end{aligned} \quad (2.12)$$

Now consider $z^\alpha = a_n^\alpha = n^\gamma \log n$ (the generalized normalization). In the case $\gamma \in [1, 2]$, the expected number of non-isolated vertices is

$$\begin{aligned} \mathbb{E}|V_n| &= n\mathbb{P}\left(\max_{i=1,\dots,n-1} X_1 X_{1+i} > a_n\right) \sim \frac{n^2}{a_n^\alpha} \int_{n/a_n^\alpha}^1 y^{-2}(1 - e^{-y}) dy \\ &\sim \frac{n^{2-\gamma}}{\log n} \int_{n^{1-\gamma}/\log n}^1 y^{-1} dy. \end{aligned} \quad (2.13)$$

In the case $\gamma \in (0, 1)$, the integral $\int_{n/a_n^\alpha}^n$ is of order $(n/a_n^\alpha)^{-1}$ and hence $\mathbb{E}|V_n| \sim n$. The case $\gamma > 2$ is clear, as $\mathbb{E}|E_n| \rightarrow 0$.

Letting $A_{n,i}$ denote the event that vertex i is not isolated and $B_{n,(i,j)}$ the event that (i, j) is an edge, the next quantity we will compute is $\rho_{n,(i,j)} = \mathbb{P}(B_{n,(i,j)} \mid A_{n,i} \cap A_{n,j})$. If this conditional probability has a limit, say $\rho_{(i,j)}$, then it may be interpreted as the probability of having an edge between two non-isolated vertices of the limit graph.

$$\begin{aligned} \mathbb{P}\left(A_{n,1} \cap A_{n,2} \cap B_{n,(1,2)}^c\right) &= 2 \int_1^\infty \alpha x_1^{-\alpha-1} dx_1 \int_1^{x_1} \alpha x_2^{-\alpha-1} dx_2 \mathbf{1}_{\{x_1 x_2 < a_n\}} \left(1 - \mathbb{P}\left(X_1 \leq \frac{a_n}{x_2}\right)^{n-2}\right) \\ &= 2 \int_1^{\sqrt{a_n}} \alpha x_2^{-\alpha-1} dx_2 \int_{x_2}^{\frac{a_n}{x_2}} \alpha x_1^{-\alpha-1} dx_1 \left(1 - \left(1 - \left(\frac{x_2}{a_n}\right)^\alpha\right)^{n-2}\right) \\ &\sim \frac{2n^2}{a_n^{2\alpha}} \int_{\frac{n}{a_n^\alpha}}^{\frac{n}{a_n^\alpha}} y_2^{-2} (1 - e^{-y_2}) dy_2 \int_{\frac{n}{a_n^\alpha}}^{\frac{n}{a_n^\alpha}} y_1^{-2} dy_1, \end{aligned} \quad (2.14)$$

where for the first equality, WLOG we assumed that $x_1 > x_2$. The indicator function constraint then gives $x_2 < \sqrt{a_n}$ in the second equality. After a change of variables: $\left(\frac{x_i}{a_n}\right)^\alpha = \frac{y_i}{n}$, a standard asymptotic study yields

$$\mathbb{P}\left(A_{n,1} \cap A_{n,2} \cap B_{n,(1,2)}^c\right) \sim \begin{cases} \frac{2}{n^{\gamma-1} \log n} & \gamma \geq 1, \\ 1 & \gamma \in (0, 1). \end{cases} \quad (2.15)$$

Complementarily,

$$\begin{aligned} \mathbb{P}\left(A_{n,1} \cap A_{n,2} \cap B_{n,(1,2)}\right) &= \int_1^\infty \alpha x_1^{-\alpha-1} dx_1 \int_1^\infty \alpha x_2^{-\alpha-1} dx_2 \mathbf{1}_{\{x_1 x_2 > a_n\}} \\ &= \int_1^{a_n} \alpha x_1^{-\alpha-1} dx_1 \int_{\frac{a_n}{x_1}}^\infty \alpha x_2^{-\alpha-1} dx_2 + \int_{a_n}^\infty \alpha x_1^{-\alpha-1} dx_1 \int_1^\infty \alpha x_2^{-\alpha-1} dx_2 \sim \frac{\gamma}{n^\gamma} \quad \text{for all } \gamma > 0. \end{aligned} \quad (2.16)$$

Combining the above results, we have $\rho_{(i,j)} = 0$ for all $\gamma > 0$.

Remark 2.3. All our estimates so far seem consistent and *suggest* that a limit random graph should exist for $\gamma \in (0, 2)$. More precisely,

- with $\gamma \in (0, 1)$, $\mathbb{E}|E_n| \sim (\mathbb{E}|V_n|)^{2-\gamma}$, and the limit graph is ‘sparse’.
- with $\gamma \in (1, 2)$, the limit graph is ‘extremely sparse’, meaning that the expected numbers of edges and vertices are of the same order.
- with $\gamma \geq 2$, contrarily, in the limit there is no random graph in distribution, as the top-2 order statistics of X_1, \dots, X_n go to zero (and hence all edges are vacant).
- The zero conditional probability of an edge connecting two non-isolated vertices may look puzzling but a possible interpretation is that, as the number of non-isolated vertices is infinite (in an appropriate sense), given any two vertices the probability of seeing an edge between them is zero.

In a similar fashion, we proceed to investigate the appearance of triangles and its variants. First is the vacant triangle probability. Given three non-isolated vertices, we find the probability that no edges are

present in-between.

$$\begin{aligned}
& \mathbb{P}\left(A_{n,1} \cap A_{n,2} \cap A_{n,3} \cap B_{n,(1,2)}^c \cap B_{n,(1,3)}^c \cap B_{n,(2,3)}^c\right) \\
&= 6 \int_1^\infty \alpha x_1^{-\alpha-1} dx_1 \int_1^{x_1} \alpha x_2^{-\alpha-1} dx_2 \int_1^{x_2} \alpha x_3^{-\alpha-1} dx_3 \\
&\quad \cdot \mathbf{1}_{\{x_1 x_2 < a_n\}} \mathbf{1}_{\{x_1 x_3 < a_n\}} \mathbf{1}_{\{x_2 x_3 < a_n\}} \left(1 - \mathbb{P}\left(X_1 \leq \frac{a_n}{x_3}\right)^{n-3}\right) \\
&= 6 \int_1^{\sqrt{a_n}} \alpha x_3^{-\alpha-1} dx_3 \int_{x_3}^{\sqrt{a_n}} \alpha x_2^{-\alpha-1} dx_2 \int_{x_2}^{\frac{a_n}{x_3}} \alpha x_1^{-\alpha-1} dx_1 \left(1 - \left(1 - \left(\frac{x_3}{a_n}\right)^\alpha\right)^{n-3}\right) \\
&\quad \sim \frac{6n^3}{a_n^{3\alpha}} \int_{\frac{n}{a_n^\alpha}}^{\frac{n}{a_n^{\alpha/2}}} y_3^{-2} (1 - e^{-y_3}) dy_3 \int_{y_3}^{\frac{n}{a_n^{\alpha/2}}} y_2^{-2} dy_2 \int_{y_2}^{\frac{n^2}{a_n^\alpha} \frac{1}{y_3}} y_1^{-2} dy_1, \quad (2.17)
\end{aligned}$$

where for the first equality, WLOG we assumed that $x_1 > x_2 > x_3$. The indicator function constraint then gives $x_2 < \sqrt{a_n}, x_3 < \sqrt{a_n}$ in the second equality. After a change of variables: $\left(\frac{x_i}{a_n}\right)^\alpha = \frac{y_i}{n}$, a standard asymptotic study yields

$$\mathbb{P}\left(A_{n,1} \cap A_{n,2} \cap A_{n,3} \cap B_{n,(1,2)}^c \cap B_{n,(1,3)}^c \cap B_{n,(2,3)}^c\right) \sim \begin{cases} \frac{3}{2n^{\gamma-1} \log n} & \gamma \geq 1, \\ 1 & \gamma \in (0, 1). \end{cases} \quad (2.18)$$

Next is the probability of there being only one edge present in-between three non-isolated vertices.

$$\begin{aligned}
& \mathbb{P}\left(A_{n,1} \cap A_{n,2} \cap A_{n,3} \cap B_{n,(1,2)} \cap B_{n,(1,3)}^c \cap B_{n,(2,3)}^c\right) \\
&= \int_1^\infty \alpha x_1^{-\alpha-1} dx_1 \int_1^\infty \alpha x_2^{-\alpha-1} dx_2 \int_1^\infty \alpha x_3^{-\alpha-1} dx_3 \\
&\quad \cdot \mathbf{1}_{\{x_1 x_2 > a_n\}} \mathbf{1}_{\{x_1 x_3 < a_n\}} \mathbf{1}_{\{x_2 x_3 < a_n\}} \left(1 - \mathbb{P}\left(X_1 \leq \frac{a_n}{x_3}\right)^{n-3}\right) \\
&= \int_1^{\sqrt{a_n}} \alpha x_3^{-\alpha-1} dx_3 \int_{x_3}^{\frac{a_n}{x_3}} \alpha x_1^{-\alpha-1} dx_1 \int_{\frac{a_n}{x_1}}^{\frac{a_n}{x_3}} \alpha x_2^{-\alpha-1} dx_2 \left(1 - \left(1 - \left(\frac{x_3}{a_n}\right)^\alpha\right)^{n-3}\right) \\
&\quad \sim \frac{n^3}{a_n^{3\alpha}} \int_{\frac{n}{a_n^\alpha}}^{\frac{n}{a_n^{\alpha/2}}} y_3^{-2} (1 - e^{-y_3}) dy_3 \int_{y_3}^{\frac{n^2}{a_n^\alpha} \frac{1}{y_3}} y_1^{-2} dy_1 \int_{\frac{n^2}{a_n^\alpha} \frac{1}{y_1}}^{\frac{n^2}{a_n^\alpha} \frac{1}{y_3}} y_2^{-2} dy_2, \quad (2.19)
\end{aligned}$$

where for the second equality, we noticed that it is impossible that $x_1 > 1, x_2 > 1, x_3 > a_n$ and yet $x_1 x_3 < a_n, x_2 x_3 < a_n$, then the indicator function constraint strengthens it further to $x_3 < \sqrt{a_n}$. After a change of variables: $\left(\frac{x_i}{a_n}\right)^\alpha = \frac{y_i}{n}$, a standard asymptotic study yields

$$\mathbb{P}\left(A_{n,1} \cap A_{n,2} \cap A_{n,3} \cap B_{n,(1,2)} \cap B_{n,(1,3)}^c \cap B_{n,(2,3)}^c\right) \sim \begin{cases} \frac{\gamma-1}{n^{2\gamma-1}} & \gamma > 1, \\ \frac{\log \log n}{n \log n} & \gamma = 1, \\ \frac{\gamma}{n^\gamma} & \gamma \in (0, 1). \end{cases} \quad (2.20)$$

Then comes the probability of a two-star.

$$\begin{aligned}
& \mathbb{P}\left(A_{n,1} \cap A_{n,2} \cap A_{n,3} \cap B_{n,(1,2)} \cap B_{n,(2,3)} \cap B_{n,(1,3)}^c\right) \\
&= \int_1^\infty \alpha x_1^{-\alpha-1} dx_1 \int_1^\infty \alpha x_2^{-\alpha-1} dx_2 \int_1^\infty \alpha x_3^{-\alpha-1} dx_3 \mathbf{1}_{\{x_1 x_2 > a_n\}} \mathbf{1}_{\{x_2 x_3 > a_n\}} \mathbf{1}_{\{x_1 x_3 < a_n\}} \\
&= \int_{\sqrt{a_n}}^{a_n} \alpha x_2^{-\alpha-1} dx_2 \int_{\frac{a_n}{x_2}}^{x_2} \alpha x_1^{-\alpha-1} dx_1 \int_{\frac{a_n}{x_2}}^{\frac{a_n}{x_1}} \alpha x_3^{-\alpha-1} dx_3 \\
&+ \int_{a_n}^\infty \alpha x_2^{-\alpha-1} dx_2 \int_1^{a_n} \alpha x_1^{-\alpha-1} dx_1 \int_1^{\frac{a_n}{x_1}} \alpha x_3^{-\alpha-1} dx_3 \\
&\sim \frac{n^3}{a_n^{3\alpha}} \int_{\frac{n}{a_n}}^n y_2^{-2} dy_2 \int_{\frac{n^2}{a_n^2} \frac{1}{y_2}}^{y_2} y_1^{-2} dy_1 \int_{\frac{n^2}{a_n^2} \frac{1}{y_1}}^{\frac{n^2}{a_n^2} \frac{1}{y_1}} y_3^{-2} dy_3 \\
&\quad + \frac{n^3}{a_n^{3\alpha}} \int_n^\infty y_2^{-2} dy_2 \int_{\frac{n}{a_n}}^n y_1^{-2} dy_1 \int_{\frac{n}{a_n}}^{\frac{n^2}{a_n^2} \frac{1}{y_1}} y_3^{-2} dy_3 \sim \frac{2}{n^\gamma \log n}, \quad (2.21)
\end{aligned}$$

where for the second equality, the indicator function constraint gives $1 < x_1 < a_n, 1 < x_3 < a_n$ and $x_1 < x_2, x_3 < x_2$, which further implies that $x_2 > \sqrt{a_n}$. Then depending on whether $x_2 < a_n$ or $x_2 > a_n$, we have different integration limits set up (first and second term in the second equality respectively). After a change of variables: $\left(\frac{x_i}{a_n}\right)^\alpha = \frac{y_i}{n}$, the conclusion readily follows from a standard asymptotic analysis.

Lastly, we show that given three non-isolated vertices, a triangle is even less likely to appear than a two-star. Note that

$$\begin{aligned}
& \mathbb{P}\left(A_{n,1} \cap A_{n,2} \cap A_{n,3} \cap B_{n,(1,2)} \cap B_{n,(2,3)}\right) \\
&= \int_1^\infty \alpha x_1^{-\alpha-1} dx_1 \int_1^\infty \alpha x_2^{-\alpha-1} dx_2 \int_1^\infty \alpha x_3^{-\alpha-1} dx_3 \mathbf{1}_{\{x_1 x_2 > a_n\}} \mathbf{1}_{\{x_2 x_3 > a_n\}} \\
&= \int_1^{a_n} \alpha x_2^{-\alpha-1} dx_2 \int_{\frac{a_n}{x_2}}^\infty \alpha x_1^{-\alpha-1} dx_1 \int_{\frac{a_n}{x_2}}^\infty \alpha x_3^{-\alpha-1} dx_3 \\
&\quad + \int_{a_n}^\infty \alpha x_2^{-\alpha-1} dx_2 \int_1^\infty \alpha x_1^{-\alpha-1} dx_1 \int_1^\infty \alpha x_3^{-\alpha-1} dx_3 \sim \frac{2}{n^\gamma \log n}, \quad (2.22)
\end{aligned}$$

where depending on $x_2 < a_n$ or $x_2 > a_n$, we have different integration limits set up for the first and second term in the second equality respectively. It is then immediate that

$$\mathbb{P}\left(A_{n,1} \cap A_{n,2} \cap A_{n,3} \cap B_{n,(1,2)} \cap B_{n,(2,3)} \cap B_{n,(1,3)}\right) = o\left(\frac{1}{n^\gamma \log n}\right). \quad (2.23)$$

Combining the above results, we conclude that as in the case of two non-isolated vertices, when there are three non-isolated vertices, the most dominant feature is a vacant triangle. Since the limit object is sparse, this is not surprising. In fact, we may generalize and show that vacant cliques are always preferred.

Remark 2.4. What is more worth noting is that the toy model introduced displays an interesting *anti-transitive* characteristic, for example concerning the appearance of triangles vs. two-stars, which is not usually captured by (dense) random graph models. A possible interpretation in terms of social networks is the following: For $\gamma \in (0, 2)$, although the number of edges (friendship relations) does not scale as the square of the number of vertices (people), both are infinite, suggesting that every person has abundant friendship opportunities in the vast network. If Person A and Person B are friends and Person B and Person C are friends, then A and C will try not to get too familiar with each other as more mutual friends will entail less privacy, which in turn contributes to the sparsity of this social network.

Recall the notion of clique and followers, and recall the definition of K_0, K_1, \dots, K_{K_0} . One could define accordingly $K_{n,0}, \dots, K_{n,K_{n,0}}$, with $K_{n,0}$ representing the number of vertices in the clique for the random graph G_n from the discrete model (based on X_1, \dots, X_n and normalization a_n) and similar definitions of

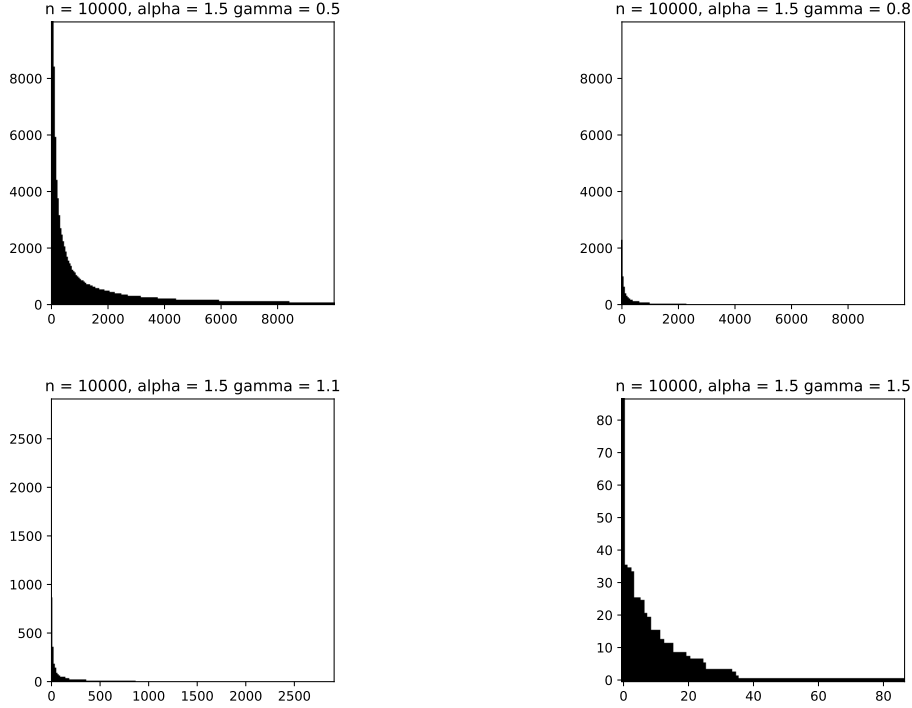


FIGURE 1. Empirical graphons of the toy example, with $\alpha = 1.5$, $\gamma = 0.5, 0.8, 1.1, 1.5$, and $n = 10000$.

$K_{n,j}$. One might for the sake of simplicity set $K_{n,j} = 0$ for all $j > K_{n,0}$. Then, $\mathbf{K}_n = \{K_{n,j}\}_{j \in \mathbb{N}_0}$ determines the structure of the random graph G_n completely.

From this point of view, all the questions that we raised earlier on the random graphs G_n are kind of ‘fake’, as they are essentially on the decreasing sequence \mathbf{K}_n . For example, the total number of vertices is $|V_n| = \sum_{j=0}^{\infty} K_{n,j}$ and the total number of edges is

$$|E_n| = \binom{K_{n,0}}{2} + \sum_{j=1}^{K_{n,0}} (K_{n,0} + 1 - j) K_{n,j}. \quad (2.24)$$

In particular, one may readily compute the number of vertices with associated values larger than $\sqrt{a_n}$. This is $\mathbb{E}K_{n,0}$, the expected number of vertices in the clique part,

$$n\mathbb{P}(X_1 > \sqrt{a_n}) = \frac{n}{a_n^{\alpha/2}} = \frac{n^{1-\gamma/2}}{\log^{1/2} n}. \quad (2.25)$$

Barring fluctuations, the order of expected edges is thus naively $n^{2-\gamma}/\log n$. Note the difference between this order and $\mathbb{E}|E_n|$ (2.9). This implies that in asymptotics, most of the edges are coming from ‘followers’. See Figure 1 for some simulations.

In Section 2.1 we studied in detail the toy model at the critical regime. It is an interesting question in extreme value theory to describe the limit behavior of \mathbf{K}_n at the sub- and super-critical regimes ($\gamma < 2$ and $\gamma > 2$ respectively), which in turn should shed light on our quest for the graph limit (if exists).

3. SUPER-CRITICAL REGIME

As was pointed out in Sections 1 and 2.2, taking the normalization $a_n = n^{2/\alpha} \log n$ relates our toy example to the anti-clustering condition for the Poisson approximations for U -statistics. Indeed, the additional $\log n$ to the critical regime $a_n = n^{2/\alpha}$ explored in Section 2.1 suggests that the entire super-critical regime ($a_n^\alpha = n^\gamma \log n$ with $\gamma > 2$, or alternatively, $a_n \gg n^{2/\alpha}$) satisfies the anti-clustering condition. Since there

is no random graph in distribution in the limit, the super-critical regime is relatively not as interesting as compared to the sub-critical regime ($a_n^\alpha = n^\gamma \log n$ with $\gamma < 2$, or alternatively, $a_n \ll n^{2/\alpha}$). The latter topic will be the central focus of Section 4. Nevertheless, the limit object for the super-critical regime captures some intriguing characteristics, as we will describe in this section.

Recall that $K_{n,0} = \sum_{i=1}^n \mathbf{1}_{\{X_i/\sqrt{a_n} > 1\}}$ denotes the number of vertices in the clique. In the critical case, as we explained earlier, the limit $K_{n,0} \rightarrow K_0$ is Poisson distributed. On the contrary, since $K_{n,0} \rightarrow 0$ in probability in the super-critical regime, only a conditional limit theorem is worth investigating in this case. Given the appearance of a non-trivial random graph, what is the conditional law $\mathcal{L}(K_{n,0} | K_{n,0} \geq 1)$? Recognizing that $K_{n,0}$ is Binomial distributed with parameter $(n, a_n^{-\alpha/2})$, the question has an easy answer.

$$\mathbb{P}(K_{n,0} \geq 1) = 1 - \left(1 - \frac{1}{a_n^{\alpha/2}}\right)^n \sim \frac{n}{a_n^{\alpha/2}} = \frac{n^{1-\gamma/2}}{\log^{1/2} n}, \quad (3.1)$$

$$\mathbb{P}(K_{n,0} = 1) = n \left(\frac{1}{a_n^{\alpha/2}}\right) \left(1 - \frac{1}{a_n^{\alpha/2}}\right)^{n-1} \sim \frac{n}{a_n^{\alpha/2}} = \frac{n^{1-\gamma/2}}{\log^{1/2} n}. \quad (3.2)$$

This is consistent with observation (2.25).

Remark 3.1. For explicitness, here we base our calculations on the toy model for the super-critical regime. We note however the above calculations could be extended to the more general framework to be introduced in Section 4, where $K_{n,0}$ is Binomial distributed with parameter $(n, \bar{F}(\sqrt{a_n}))$, and

$$\mathbb{E}K_{n,0} = n\bar{F}(\sqrt{a_n}) \rightarrow 0 \quad (3.3)$$

at the super-critical regime, i.e., with $\bar{F}(\sqrt{a_n})$ taking the place of $a_n^{-\alpha/2}$. We will elaborate upon this general framework in the more intriguing sub-critical regime in Section 4, where a limit random graph does exist.

We conclude that the clique part (conditioning on non-empty) typically only contains one vertex. There is a fine point when computing the probability that $K_{n,0} = 1$ though. This event does not necessarily imply the appearance of a star graph as the edge number may still be zero. We demonstrate this subtlety below.

$$\begin{aligned} \mathbb{P}(\text{clique vertex} = 1) &= n \int_{\sqrt{a_n}}^{a_n} \alpha x_1^{-\alpha-1} dx_1 \left[\left(1 - \frac{1}{a_n^{\alpha/2}}\right)^{n-1} - \left(1 - \left(\frac{x_1}{a_n}\right)^\alpha\right)^{n-1} \right] \\ &\quad + n \int_{a_n}^{\infty} \alpha x_1^{-\alpha-1} dx_1 \left(1 - \frac{1}{a_n^{\alpha/2}}\right)^{n-1}. \end{aligned} \quad (3.4)$$

Here we eliminate the situation where $K_{n,0} = 1$, but no edge is formed between the clique vertex X_1 and the follower vertices X_2, \dots, X_n . The scalar n indicates that the clique could be centered at any vertex. The second term on the right is of order $na_n^{-\alpha} \ll n^{1-\gamma}$, while the first term, after a change of variables: $\left(\frac{x_1}{a_n}\right)^\alpha = \frac{y_1}{n}$, asymptotically becomes

$$\frac{n^2}{a_n^\alpha} \int_{\frac{n}{a_n^{\alpha/2}}}^n y_1^{-2} (1 - e^{-y_1}) dy_1 \sim \frac{n^2}{a_n^\alpha} \log\left(\frac{a_n^{\alpha/2}}{n}\right) \sim \left(\frac{\gamma}{2} - 1\right) n^{2-\gamma}. \quad (3.5)$$

Combined, this gives the correct probability of a star graph with a lone vertex in the clique as $(\gamma/2 - 1)n^{2-\gamma}$, which is smaller than (3.1) (3.2).

Let us delve deeper into the structure of this star graph. On average how many follower vertices are connected to the clique? Notice that $K_{n,1}$ by itself counts the number of followers in this case; $K_{n,j} = 0$ for all $j > 1$ automatically by construction. The answer then comes fast.

$$\begin{aligned} \mathbb{P}(\text{clique vertex} = 1, K_{n,1} = 1) &= n(n-1) \int_{\sqrt{a_n}}^{a_n} \alpha x_1^{-\alpha-1} dx_1 \int_{\frac{a_n}{x_1}}^{\sqrt{a_n}} \alpha x_2^{-\alpha-1} dx_2 \left(1 - \left(\frac{x_1}{a_n}\right)^\alpha\right)^{n-2} \\ &\sim \frac{n^2}{a_n^\alpha} \int_{\frac{n}{a_n^{\alpha/2}}}^n y_1^{-1} e^{-y_1} dy_1 \sim \frac{n^2}{a_n^\alpha} \log\left(\frac{a_n^{\alpha/2}}{n}\right) \sim \left(\frac{\gamma}{2} - 1\right) n^{2-\gamma}. \end{aligned} \quad (3.6)$$

Here the scalars n and $n - 1$ in the equality indicate that the clique could be centered at any vertex and the follower could come from any of the remaining vertices. A standard asymptotic analysis then yields the asymptotic order after a change of variables: $\left(\frac{x_1}{a_n}\right)^\alpha = \frac{y_1}{n}$. This probability is asymptotically the same as having a lone clique star graph that was established previously. We state this finding.

Proposition 3.2. Consider the toy model at the super-critical regime ($a_n^\alpha = n^\gamma \log n$ with $\gamma > 2$). Given that the graph is non-empty, in the limit predominantly it has exactly two vertices, one clique vertex and one follower vertex.

A physical interpretation of this phenomenon might be the following: For a typical behavior, with probability going to one we would not see any graph eventually. In the rare event that we do see one, we would need certain ‘extra energy’ (than typical) to push some of the X_i values up, and the most ‘economical’ way to do so is to push one up to the clique and another up to be a follower. Pushing up two to the clique or pushing up more than one follower or any other construction, by comparison, might be too costly.

4. SUB-CRITICAL REGIME

The prototype example presented in Section 2 may be generalized. We consider a generic situation where $\{X_n\}_{n \in \mathbb{N}}$ are i.i.d. non-negative random variables with tail distribution

$$\bar{F}(x) = \mathbb{P}(X_1 > x) = x^{-\alpha} L(x), \quad (4.1)$$

where L is a slowly varying function at infinity, i.e., $L(cx)/L(x) \rightarrow 1$ as $x \rightarrow \infty$ for every $c > 0$. In a complementary manner, we also write the cumulative distribution function $F(x) = \mathbb{P}(X_1 \leq x)$. Let $\{a_n^*\}_{n \in \mathbb{N}}$ be any sequence such that

$$\lim_{n \rightarrow \infty} n \bar{F}(\sqrt{a_n^*}) = 1. \quad (4.2)$$

It may be verified that the three regimes correspond to

- Super-critical regime: $a_n^* = o(a_n)$.
- Critical regime: $a_n \sim a_n^*$.
- Sub-critical regime: $a_n = o(a_n^*)$.

Remark 4.1. Such regularly varying tail distributions can be extended to product-type functions as in the toy example. Write $\bar{F}_2(x) = \mathbb{P}(X_1 X_2 > x)$. For example, in the case that $\mathbb{E}X_1^\alpha = \infty$, we have

$$\bar{F}(x) = o(\bar{F}_2(x)). \quad (4.3)$$

Let $\{a_{2,n}^*\}_{n \in \mathbb{N}}$ be any sequence such that

$$\lim_{n \rightarrow \infty} n \bar{F}_2(\sqrt{a_{2,n}^*}) = 1. \quad (4.4)$$

Then $a_n^* = o(a_{2,n}^*)$. (See [10, Lemma 4.1] for relevant discussions.)

We will investigate the limit graph at the sub-critical regime under the above generic assumptions. For ease of notation, let $K_n \equiv K_{n,0} = \sum_{i=1}^n \mathbf{1}_{\{X_i/\sqrt{a_n} > 1\}}$ denote the number of vertices in the clique. In the sub-critical regime, we assume throughout that $a_n = o(a_n^*)$, or equivalently

$$\sigma_n^2 := \mathbb{E}K_n = n \bar{F}(\sqrt{a_n}) \rightarrow \infty. \quad (4.5)$$

Since K_n is Binomial distributed with parameter $(n, \bar{F}(\sqrt{a_n}))$, $K_n \sim \sigma_n^2$ in probability, and the random variable K_n is well-concentrated around σ_n^2 .

Introduce two i.i.d. sequences of random variables $\{Y_{n,i}\}_{i \in \mathbb{N}}$ and $\{Z_{n,i}\}_{i \in \mathbb{N}}$ with

$$\mathbb{P}(Y_{n,1} > y) = \frac{\bar{F}(y\sqrt{a_n})}{\bar{F}(\sqrt{a_n})} \sim y^{-\alpha}, \text{ as } n \rightarrow \infty \text{ for all } y > 1, \quad (4.6)$$

$$\mathbb{P}(Z_{n,1} \leq x) = \frac{F(x)}{F(\sqrt{a_n})}, \text{ } x \in (0, \sqrt{a_n}]. \quad (4.7)$$

In other words, $\{Y_{n,i}\}_{i \in \mathbb{N}}$ are i.i.d. with law as $\mathcal{L}(X_1 | X_1 > \sqrt{a_n})$ (with scaling adjustment) and $\{Z_{n,i}\}_{i \in \mathbb{N}}$ are i.i.d. with law as $\mathcal{L}(X_1 | X_1 \leq \sqrt{a_n})$. Assume further that these two sequences are independent. Then for every $n \in \mathbb{N}$, given K_n , the values of $\{X_i\}_{i=1, \dots, n}$ corresponding to those larger than (less than resp.) the

threshold $\sqrt{a_n}$ share the same joint law of $Y_{n,1}, \dots, Y_{n,K_n}$ ($Z_{n,1}, \dots, Z_{n,n-K_n}$, resp.). We order $\{Y_{n,i}\}_{i=1, \dots, K_n}$ in *increasing* order statistics

$$Y_{n,K_n:K_n} > \dots > Y_{n,1:K_n} > \sqrt{a_n} > \frac{a_n}{Y_{n,1:K_n}} > \dots > \frac{a_n}{Y_{n,K_n:K_n}}, \quad (4.8)$$

where listed on the right hand side are the thresholds for different groups of followers.

Define the statistics

$$\tau_n(x) := \frac{a_n}{Y_{n, \lceil xK_n \rceil : K_n}}, \quad x \in (0, 1). \quad (4.9)$$

We are interested in the asymptotic behavior of the height function

$$H_n(x) := \sum_{i=1}^{n-K_n} \mathbf{1}_{\{Z_{n,i} > \tau_n(x)\}}. \quad (4.10)$$

This construction associates the law of $H_n(x)$ to that of the number of not-in-clique vertices that are connected to the vertices in the clique corresponding to those top $\lceil xK_n \rceil$ -values of $\{Y_{n,i}\}_{i=1, \dots, K_n}$. At one end, $H_n(1)$ is the number of followers of the leader from the clique, i.e., $n - K_n$, thus $H_n(1) \sim n$ with high probability. At the other end, we take $H_n(0) \equiv 0$ by convention. For notational convenience, set

$$B_{n,i}(x) := \mathbf{1}_{\{Z_{n,i} > \tau_n(x)\}}. \quad (4.11)$$

We are now ready to state our main result, which says that the limit fluctuation of the height function has two independent components, one as a generalized Brownian bridge, the other as a time-changed Brownian motion.

Theorem 4.2. Assume (4.5). Assume that, in addition to (4.1), the i.i.d. random variables X_i have a continuous probability density function $f \in RV_{-\alpha-1}$. We have, for $\theta_n(x)$ defined as (4.23) below,

$$\frac{1}{\sigma_n} \{H_n(x) - \sigma_n^2 \cdot (\theta_n(1-x) - 1)\}_{x \in [0,1]} \xrightarrow{f.d.d.} \{\mathbb{B}_{x/(1-x)} + \mathbb{G}_x\}_{x \in [0,1]}, \quad (4.12)$$

where $\{\mathbb{B}_t\}_{t \in [0, \infty)}$ is a standard Brownian motion, $\{\mathbb{G}_x\}_{x \in [0,1]}$ is a generalized Brownian bridge with covariance function

$$\text{Cov}(\mathbb{G}_x, \mathbb{G}_y) = \frac{\min(x, y)(1 - \max(x, y))}{(1-x)^2(1-y)^2}, \quad x, y \in [0, 1), \quad (4.13)$$

and \mathbb{B} and \mathbb{G} are independent.

Note that throughout, the index x is strictly less than 1 (covariance explodes as $x \uparrow 1$). On the other hand, convergence at $x = 0$ is clear, as both sides equal zero. We shall see later that $\theta_n(1-x) \rightarrow (1-x)^{-1}$. However, one cannot simply replace the centering $\theta_n(1-x)$ in (4.12) by $(1-x)^{-1}$ unless under a very strong assumption on the law of X_i . See Remark 4.4. We refer to the toy model in Section 2, $\overline{F}(x) = x^{-\alpha}$, $x > 1$, for an example where the assumption is satisfied. The regularly varying function in (4.1) thus introduces a bias in general for limit fluctuations.

We shall decompose H_n further and identify the relevant contribution from the different parts of the statistics to \mathbb{B} and \mathbb{G} . For this purpose, we introduce $\mathcal{K}_n := \sigma(K_n, Y_{n,1}, \dots, Y_{n,K_n})$, and

$$\widehat{p}_n(x) := \mathbb{P}(Z_{n,i} > \tau_n(x) \mid \mathcal{K}_n) \quad \text{and} \quad p_n(x) := \frac{\overline{F}(\sqrt{a_n})}{F(\sqrt{a_n})} (\theta_n(1-x) - 1), \quad (4.14)$$

and write

$$\begin{aligned} \overline{H}_n(x) &= \sum_{i=1}^{n-K_n} (B_{n,i}(x) - p_n(x)) \\ &= \sum_{i=1}^{n-K_n} (B_{n,i}(x) - \widehat{p}_n(x)) + (n-K_n)(\widehat{p}_n(x) - p_n(x)) =: \overline{H}_{1,n}(x) + \overline{H}_{2,n}(x). \end{aligned} \quad (4.15)$$

We will show that $\sigma_n^{-1} \overline{H}_{1,n}$ and $\sigma_n^{-1} \overline{H}_{2,n}$ converge to \mathbb{B} and \mathbb{G} , respectively. The convergence is actually stronger than finite-dimensional distributions. We first examine $\overline{H}_{2,n}$.

Lemma 4.3. With the notations above, under the assumptions in Theorem 4.2, we have

$$\frac{n}{\sigma_n} \{\widehat{p}_n(x) - p_n(x)\}_{x \in (0,1)} \xrightarrow{f.d.d.} \{\mathbb{G}_x\}_{x \in (0,1)}. \quad (4.16)$$

Proof. We begin the analysis of asymptotics by first examining the i.i.d. $Y_{n,i}$. Definition (4.6) implies that $Y_{n,1} \Rightarrow U^{-1/\alpha}$, where U is a uniform random variable on $(0,1)$. Set $Y_{n,i} = W_{n,i}^{-1}$ and $W_n \equiv W_{n,1}$. We need some background on quantile processes [12, 13]. Following notations from earlier, let F_Z be the cumulative distribution function of a random variable Z and \overline{F}_Z its tail probability function. Let F_Z^{-1} denote the left-continuous inverse function of F_Z . Let $\mathbb{F}_{Z,n}^{-1}(x)$ denote the quantile process of i.i.d. copies Z_1, \dots, Z_n . It follows that $\mathbb{F}_{Z,n}^{-1}(x) = Z_{[xn]:n}$, where $Z_{i:n}$ is the i th smallest order statistics of Z_1, \dots, Z_n . Then $F_{W_n}(W_n)$ is a uniform random variable, and for all $m_n \rightarrow \infty$,

$$\sqrt{m_n} \{\mathbb{Q}_{n,m_n}(x) - x\}_{x \in [0,1]} \equiv \sqrt{m_n} \{F_{W_n} \circ \mathbb{F}_{W_n, m_n}^{-1}(x) - x\}_{x \in [0,1]} \Rightarrow \{\mathbb{B}_x^{br}\}_{x \in [0,1]}. \quad (4.17)$$

Here, $\{\mathbb{B}_x^{br}\}_{x \in [0,1]}$ is a standard Brownian bridge, a centered Gaussian process with

$$\text{Cov}(\mathbb{B}_x^{br}, \mathbb{B}_y^{br}) = \min(x, y)(1 - \max(x, y)), \quad x, y \in [0, 1] \quad (4.18)$$

in $D([0, 1])$. $\mathbb{Q}_{n,m_n}(x)$ so defined has the law of the quantile process of m_n i.i.d. uniform random variables. Furthermore, from (4.9),

$$\tau_n(x) = \sqrt{a_n} \mathbb{F}_{W_n, K_n}^{-1}(1 - x). \quad (4.19)$$

Combining the above observations, we have

$$\widehat{p}_n(x) = \frac{\overline{F}(a_n/Y_{n, [xK_n]:K_n}) - \overline{F}(\sqrt{a_n})}{F(\sqrt{a_n})} = \widehat{\rho}_n(x) \frac{\overline{F}(\sqrt{a_n})}{F(\sqrt{a_n})}, \quad (4.20)$$

with

$$\widehat{\rho}_n(x) = \frac{\overline{F}(\sqrt{a_n} \mathbb{F}_{W_n, K_n}^{-1}(1 - x))}{\overline{F}(\sqrt{a_n})} - 1. \quad (4.21)$$

We rewrite $\widehat{\rho}_n$ as a function of $\mathbb{Q}_n \equiv \mathbb{Q}_{n, K_n}$. Namely,

$$\begin{aligned} \widehat{\rho}_n(x) &= \frac{\overline{F}(\sqrt{a_n} F_{W_n}^{-1} \circ F_{W_n} \circ \mathbb{F}_{W_n, K_n}^{-1}(1 - x))}{\overline{F}(\sqrt{a_n})} - 1 \\ &= \frac{\overline{F}(\sqrt{a_n} F_{W_n}^{-1} \circ \mathbb{Q}_n(1 - x))}{\overline{F}(\sqrt{a_n})} - 1 = \theta_n(\mathbb{Q}_n(1 - x)) - 1, \end{aligned} \quad (4.22)$$

with

$$\theta_n(x) := \frac{\overline{F}(\sqrt{a_n} F_{W_n}^{-1}(x))}{\overline{F}(\sqrt{a_n})}. \quad (4.23)$$

For the sake of simplicity, we first consider the case of (exact) power-law distribution, $\overline{F}(x) = (x \vee 1)^{-\alpha}$, $F_{W_n}^{-1}(x) = x^{1/\alpha}$, $F_{W_n}(x) = x^\alpha$, $x \in (0, 1)$. Hence

$$\theta_n(x) = \begin{cases} x^{-1} & x > \overline{F}(\sqrt{a_n}) = a_n^{-\alpha/2}, \\ a_n^{\alpha/2} & x \leq a_n^{-\alpha/2}, \end{cases} \quad (4.24)$$

and $\theta'_n(x) = -x^{-2}$ for all $x > 0$ for n large enough. This gives

$$\frac{n}{\sigma_n} (\widehat{p}_n(x) - p_n(x)) = \frac{1}{F(\sqrt{a_n})} \cdot \frac{\sigma_n}{\sqrt{K_n}} \cdot \sqrt{K_n} (\theta_n(\mathbb{Q}_n(1 - x)) - \theta_n(1 - x)). \quad (4.25)$$

A standard application of the delta method applied to (4.17) and (4.25) then yields the desired weak convergence.

Next, without assuming the exact power-law density for X_i , but simply (4.1) and that F is continuous, it still follows that $\lim_{n \rightarrow \infty} F_{W_n}^{-1}(x) = x^{1/\alpha}$, and hence

$$\lim_{n \rightarrow \infty} \theta_n(x) = x^{-1}, \quad x \in (0, 1]. \quad (4.26)$$

Assume in addition that F has a density function $f(x) \in RV_{-\alpha-1}$, we have

$$\theta'_n(x) = -\frac{f(\sqrt{a_n}F_{W_n}^{-1}(x))}{\bar{F}(\sqrt{a_n})} \frac{\sqrt{a_n}}{F'_{W_n}(F_{W_n}^{-1}(x))}. \quad (4.27)$$

We inspect the density of W_n ,

$$\begin{aligned} F'_{W_n}(x) &= \frac{f(\sqrt{a_n}/x)}{\bar{F}(\sqrt{a_n})} \frac{\sqrt{a_n}}{x^2} = \frac{f(\sqrt{a_n}/x)}{\bar{F}(\sqrt{a_n}/x)} \frac{\bar{F}(\sqrt{a_n}/x)}{\bar{F}(\sqrt{a_n})} \frac{\sqrt{a_n}}{x^2} \\ &\sim \alpha(\sqrt{a_n}/x)^{-1} \cdot x^\alpha \cdot \frac{\sqrt{a_n}}{x^2} = \alpha x^{\alpha-1}, \quad x \in (0, 1), \end{aligned} \quad (4.28)$$

where in the ' \sim ' step we applied the Karamata theorem [11, Theorem 2.1]. Furthermore, since both f and \bar{F} are regularly varying at infinity with negative index, it is known that the ' \sim ' step is uniform in x over compact intervals in $(0, 1)$ [11, Proposition 2.4]. Then,

$$\theta'_n(x) \sim - (F_{W_n}^{-1}(x))^{-2\alpha} \rightarrow -x^{-2} \quad (4.29)$$

is also uniform in x over $[a, b]$ for any $0 < a < b < 1$. So the delta method still applies to (4.17) and (4.25). \square

Remark 4.4. In the general case that X_i has a regularly-varying distribution, in (4.25) we would need $|\theta_n(1-x) - (1-x)^{-1}| = o(\sigma_n)$ in order to replace the centering $\theta_n(1-x)$ by $(1-x)^{-1}$. This is quite a strong assumption.

The examination of $\bar{H}_{1,n}$ comes next. Following Shorack [13] we can actually construct, on a different probability space, for each $n \in \mathbb{N}$ copies $\{\tilde{Y}_{n,i}, \tilde{K}_n\}_{i \in \mathbb{N}}$ of $\{Y_{n,i}, K_n\}_{i \in \mathbb{N}}$, such that $\tilde{K}_n \sim \sigma_n^2$ almost surely, and the convergence (4.17) is in the almost sure sense. Note that this coupling construction does not necessarily imply that the joint laws of $(\tilde{Y}_{n,i}, \tilde{Y}_{m,j})$ are the same as $(Y_{n,i}, Y_{m,j})$ for $m \neq n$, but we will not need such joint laws in the sequel. For ease of notation, we still let $Y_{n,i}, W_{n,i}, K_n, \tau_n(x)$ denote $\tilde{Y}_{n,i}, \tilde{W}_{n,i}, \tilde{K}_n, \tilde{\tau}_n(x)$ respectively, and emphasize that we are working on this different probability space simply by saying *for the coupled model*. Recall that $\mathcal{K}_n := \sigma(K_n, Y_{n,1}, \dots, Y_{n,K_n})$. Further define $\mathcal{K} := \sigma(\{\mathcal{K}_n\}_{n \in \mathbb{N}})$ for the coupled model. We also continue to assume $Z_{n,i}$ as before, independent from all other random variables discussed so far.

We start by noticing that for each $n \in \mathbb{N}$, given \mathcal{K}_n , $\{B_{n,i}(x)\}_{i \in \mathbb{N}}$ are i.i.d. Bernoulli random variables with parameter $\hat{p}_n(x)$ for every x . Moreover, they are nested in the sense that $B_{n,i}(x) = 1$ implies $B_{n,i}(y) = 1$ for all $y \in (x, 1)$. We fix $x \in (0, 1)$ (there is nothing to prove for $x = 0$). Then, conditioning on \mathcal{K}_n , for each $n \in \mathbb{N}$,

$$\bar{H}_{1,n}(x) = \sum_{i=1}^{n-K_n} (B_{n,i}(x) - \hat{p}_n(x)) \quad (4.30)$$

is a partial sum of (centralized) i.i.d. Bernoulli random variables with parameter $\hat{p}_n(x)$. Now, from (4.17), we know that

$$\mathbb{Q}_n(x) \equiv F_{W_n} \circ \mathbb{F}_{W_n, K_n}^{-1}(x) \rightarrow x \text{ almost surely,} \quad (4.31)$$

and $\lim_{n \rightarrow \infty} F_{W_n}(x) = x^\alpha$ for $x \in (0, 1)$. Therefore, the conditional variance is

$$\begin{aligned} (n - K_n)\hat{p}_n(x)(1 - \hat{p}_n(x)) &\sim n\bar{F}(\sqrt{a_n})\hat{p}_n(x) = n\bar{F}(\sqrt{a_n})(\theta_n(\mathbb{Q}_n(1-x)) - 1) \\ &\sim \sigma_n^2 \left(\frac{1}{1-x} - 1 \right) = \sigma_n^2 \left(\frac{x}{1-x} \right), \end{aligned} \quad (4.32)$$

almost surely, where in the last step we used the coupling $\mathbb{Q}_n(x) \rightarrow x$ almost surely and $\lim_{n \rightarrow \infty} \theta_n(x) = x^{-1}$. Then, by the central limit theorem for triangular arrays of i.i.d. random variables, we have that

$$\mathcal{L} \left(\frac{1}{\sigma_n} \bar{H}_{1,n}(x) \mid \mathcal{K} \right) \rightarrow \mathcal{L} \left(\mathcal{N} \left(0, \frac{x}{1-x} \right) \right) \text{ a.s.} \quad (4.33)$$

The above statement is interpreted as *almost-sure weak convergence*, meaning that

$$\lim_{n \rightarrow \infty} \mathbb{E} \left[\phi \left(\frac{1}{\sigma_n} \overline{H}_{1,n}(x) \right) \middle| \mathcal{K} \right] = \mathbb{E} \phi \left(\left(\frac{x}{1-x} \right)^{1/2} Z \right)$$

almost surely for all continuous and bounded functions $\phi : \mathbb{R} \rightarrow \mathbb{R}$, (4.34)

where Z on the right hand side is a standard Gaussian random variable. We shall use $\mathcal{L}_{f.d.d.}(\{\sigma_n^{-1} \overline{H}_{1,n}(x)\}_{x \in [0,1]} \mid \mathcal{K})$ in Lemma 4.5 below for the corresponding *almost-sure weak convergence of finite-dimensional distributions* of $\overline{H}_{1,n}$.

This argument can be readily extended to the multivariate central limit theorem, and it suffices to compute the covariance. Alternatively, by a standard Poissonization argument one sees immediately that the limit Gaussian process has independent increments. So, the limits of finite-dimensional distributions of $\{\sigma_n^{-1} \overline{H}_{1,n}(x)\}_{x \in [0,1]}$ are the corresponding ones of $\mathbb{B}_{x/(1-x)}$. We have thus proved the following.

Lemma 4.5. For the coupled model, with the regular variation assumption (4.1) on F and that F is continuous alone, we have

$$\mathcal{L}_{f.d.d.} \left(\frac{1}{\sigma_n} \{\overline{H}_{1,n}(x)\}_{x \in [0,1]} \middle| \mathcal{K} \right) \rightarrow \mathcal{L}_{f.d.d.} (\{\mathbb{B}_{x/(1-x)}\}_{x \in [0,1]}) \text{ a.s.}, \quad (4.35)$$

where the interpretation of the above expression is explained right after (4.34).

Remark 4.6. Note that for the limit fluctuations of $\overline{H}_{1,n}$, we do not need the central limit theorem for \mathbb{Q}_n , nor the delta method as in Lemma 4.3 (for the limit fluctuations of $\overline{H}_{2,n}$). Therefore, we do not need F to have a regularly varying density.

Proof of Theorem 4.2. Combining Lemmas 4.3 and 4.5 we obtain immediately that

$$\frac{1}{\sigma_n} \{\overline{H}_n(x)\}_{x \in [0,1]} \xrightarrow{f.d.d.} \{\mathbb{B}_{x/(1-x)} + \mathbb{G}_x\}_{x \in [0,1]}. \quad (4.36)$$

However, $\sigma_n^{-1} \overline{H}_n(x)$ has a slightly different centering from the one in Theorem 4.2, and the difference is

$$\begin{aligned} \frac{1}{\sigma_n} (\sigma_n^2 (\theta_n(1-x) - 1) - (n - K_n) p_n(x)) &= \frac{1}{\sigma_n} ((n - \mathbb{E}K_n) p_n(x) - (n - K_n) p_n(x)) \\ &= \frac{K_n - \mathbb{E}K_n}{\sigma_n} p_n(x), \end{aligned} \quad (4.37)$$

which converges to zero in L^2 . □

Recall that $\sigma_n^2 = \mathbb{E}K_n$ denotes the average number of vertices in the clique. From Theorem 4.2, we may deduce that

$$\begin{aligned} \mathbb{E}H_n(x) &\sim \sigma_n^2 \frac{x}{1-x}, \\ \text{Var}(H_n(x)) &\sim \sigma_n^2 \frac{x}{1-x} \left(1 + \frac{1}{(1-x)^2} \right). \end{aligned} \quad (4.38)$$

Since we established the theorem using increasing order statistics, this introduces a simple transformation $x \mapsto 1-x$ to the simulations in Figure 1 (drawn for the prototype toy model). Then for $x \in (0, 1]$,

$$h(x) := 1 + \lim_{n \rightarrow \infty} \frac{\mathbb{E}H_n(x)}{\sigma_n^2} = \frac{1}{x} \quad (4.39)$$

should give the boundary line in question, where the extra 1 in the above expression comes from the clique-clique contribution. This is a universal result independent of the parameters. Having the same asymptotic order for the expected value and the variance of the height function $H_n(x)$ also explains why the simulations look so regular.

5. ON MODES OF GRAPH CONVERGENCE

This section aims to put our investigation into the context of random graph limits. We will see that our model serves as an uncovered boundary case between different types of graph convergence. Broadly speaking, there are three modes of convergence for exchangeable random graphs. We summarize them below. The first one is for dense graphs, and the latter two are for sparse graphs.

- (i) The one for dense graphs is the convergence of empirical graphon W_n (the graphon representation of a graph on n vertices) to some W , and it may be characterized in terms of the *cut metric* $\delta_{\square}(W_n, W) \rightarrow 0$ (in probability, and can be strengthened to almost surely under appropriate conditions) [5]. The scaling is such that each edge is represented by value 1 over a square of side length $1/n$. There are generalized versions of this type of convergence for weighted graphs, but the principal ideas are the same.
- (ii) Borgs et al. [4] introduced a type of convergence for sparse graphs, characterized by the *rescaled cut metric* δ_{\square}^r . To accommodate graphs with different edge densities, before comparing their corresponding graphons, each graphon representation W is first rescaled to W^r by

$$W^r := \|W\|_1^{-1} W \tag{5.1}$$

(i.e., multiply the weight of each edge by $\|W\|_1^{-1}$). The rescaled graphon is still in $L^1([0, 1]^2)$, but now it takes values in $[0, \infty)$. Note that for sparse graphs this scaling of the edges is appropriate, as it produces a constant order $\|W^r\|_1$. If we rescale W so that $\|W^r\|_1 = o(1)$ then automatically its cut norm (which is upper bounded by the L^1 -norm) is negligible. There are generalized versions of this type of convergence for weighted graphs, as well as to L^p graphons.

- (iii) Borgs et al. [2] introduced another type of convergence for sparse graphs, characterized by the *stretched cut metric* δ_{\square}^s . This time, each graphon is first stretched to W^s by

$$W^s(x, y) := W\left(\|W\|_1^{1/2} x, \|W\|_1^{1/2} y\right) \tag{5.2}$$

for valid x, y values. Upon stretching of the arguments of the graphon W , the resulting graphon W^s is in $L^1([0, \infty)^2)$ and $\|W^s\|_1 = 1$. Under this rescaling of the measure approach, graphons on σ -finite measure spaces of infinite total measure may be considered as limiting objects for sequences of sparse graphs, similarly as graphons on probability spaces are considered limits of dense graphs. Again there are further generalizations for this type of convergence.

Remark 5.1. In the sub-critical regime $\gamma \in (0, 2)$, our toy example in Section 2 does not fit exactly into any of the three categories of graph convergence presented above. We briefly explain why. The generated graph is not dense and so convergence mode (i) does not apply. It is also clear that reweighting the graphon (5.1) as in convergence mode (ii) does not lead to any non-trivial limit. Following explanations at the end of Section 4 and in view of the simulations in Figure 1, the limit graphon corresponds to the function $W(x, y) = \mathbf{1}_{\{xy \leq 1\}}$, $x, y \in (0, \infty)$. This mode of convergence feels very close to the stretched convergence mode (iii). Indeed, let W_n denote the graphon of our model with n vertices without scaling (a $\{0, 1\}$ -valued function on $[0, n]^2$). We essentially proved that

$$W'_n(x, y) = W_n(\mathbb{E}K_{n,0} \cdot x, \mathbb{E}K_{n,0} \cdot y) \tag{5.3}$$

has the deterministic limit $W(x, y)$, with boundary line $y = 1/x$. (See Theorem 4.2 and the accompanying remarks.) Our stretching acts in a similar way as in (5.2), *but by a slightly different stretching order*, as $\|W_n\|_1 = \mathbb{E}|E_n| \sim (\gamma/2)n^{2-\gamma}$ (2.9) while $\mathbb{E}K_{n,0} \sim na_n^{-\alpha/2} \sim n^{1-\gamma/2}/(\log n)^{1/2}$ (2.25). So there is an extra log term in our stretching as compared to (5.2). Furthermore, contrary to convergence mode (iii), the limit graphon W is not integrable. The prototype toy model therefore may be viewed as an example that lies at the boundary between rescaled convergence and stretched convergence.

Remark 5.2. We recognize that a motivating example in [4] is closely related to our toy example after a simple transformation. They consider a discrete graph of n vertices and connect vertices i, j with probability

$$\min\left\{1, n^{\beta}/(ij)^{\alpha'}\right\} = \min\left\{1, n^{\beta-2\alpha'}(i/n)^{-\alpha'}(j/n)^{-\alpha'}\right\} \tag{5.4}$$

for some parameters α' and β . In other words, the connection probability behaves like $(ij)^{-\alpha'}$, but boosted by a factor of n^{β} in case it becomes too small. Take $\alpha' = 1/\alpha$. For our toy model, roughly speaking, this

corresponds to connecting two (normalized) vertices i, j with probability

$$\min \left\{ 1, n^{\beta-2/\alpha} X_i X_j \right\} = \min \left\{ 1, \frac{X_i X_j}{a_n} \right\} \quad \text{with} \quad a_n = n^{-\beta+2/\alpha}. \quad (5.5)$$

They are interested in the case $\alpha > 1$ and $\beta \in (0, 2/\alpha)$, which avoids having almost all the edges between a sub-linear number of vertices and ensures that the cut-off from taking the minimum with 1 affects only a negligible fraction of the edges. This is exactly our sub-critical regime $a_n \ll n^{2/\alpha}$.

Now compare their edge connection probability against ours $\mathbf{1}_{\{X_i X_j / a_n > 1\}}$. So, for every edge that our model connects, they connect them too. Call these ‘hard edges’. However they are not that strict with those edges that we drop. Instead they choose whether to connect them or not depending on a Bernoulli sampling probability strictly between $(0, 1)$. Call these ‘Bernoulli edges’. They claim that after rescaling the corresponding limit graphon is $W(x, y) = (xy)^{-1/\alpha}$, which lies in $L^p([0, 1]^2)$ for $p < \alpha$, so there is no universality and the parameter influence stays in the limit. The qualitative difference between the limit graph structures in their example vs. our example is essentially due to the presence of Bernoulli edges, as the number of those edges is of larger order than the number of deterministic ones.

Taking into account the remarks above, we spell out the details in obtaining the limit graphon when Bernoulli edges are present. The mechanism will point to more underlying connections between the two models (with/without Bernoulli edges). As in our toy example, we order the vertices in the motivating example in [4] and connect vertices i, j with probability

$$p_n(i, j) := \min \left\{ 1, \frac{X_{i:n} X_{j:n}}{a_n} \right\}, \quad (5.6)$$

where $X_{1:n} > \dots > X_{n:n}$ are the order statistics of X_1, \dots, X_n . Let $\{E_{i,j}\}_{1 \leq i < j \leq n}$ be Bernoulli random variables with parameter $p_n(i, j)$, conditionally independent given $\{X_i\}_{i=1, \dots, n}$, and $E_{i,j} = E_{j,i}$. Alternatively, $E_{i,j} = 1$ if two vertices i, j (after relabeling depending on the order statistics) are connected, but the respective edge connection probability differs according to $p_n(i, j)$. Set

$$W_n(x, y) := \frac{1}{c_n} E_{[\lceil xn \rceil, \lceil yn \rceil]}, \quad (5.7)$$

for the rescaled empirical graphon, where c_n is a scaling parameter. The result in [4] (for more details see [3, Example 3.3.3]) says that for $1/\alpha = \alpha' \in (0, 1)$ and $\beta \in (0, 2\alpha')$ (which translates to our sub-critical regime $\gamma < 2$),

$$\lim_{n \rightarrow \infty} W_n(x, y) = (1 - \alpha')^2 (xy)^{-\alpha'}, \quad x, y \in (0, 1), \quad (5.8)$$

or equivalently,

$$\lim_{n \rightarrow \infty} \frac{1}{n^2 c_n} \sum_{i=1}^{\lceil xn \rceil} \sum_{j=1}^{\lceil yn \rceil} E_{i,j} = \lim_{n \rightarrow \infty} \int_0^x \int_0^y W_n(v, w) dv dw = \int_0^x \int_0^y (1 - \alpha')^2 (vw)^{-\alpha'} dv dw = (xy)^{1-\alpha'}, \quad (5.9)$$

both in an appropriate sense (in L^p for $p < 1/\alpha'$). The limit theorem established for $H_n(x)$ in our toy model (without Bernoulli edges) then corresponds to the limit of a single summation for j which runs from 1 to $\lceil n \rceil$ with $i = \lceil xK_{n,0} \rceil$.

6. FURTHER DISCUSSIONS: POWER-LAW RANDOM GRAPH WITH BERNOULLI EDGES

Expanding upon Section 5, let us take a closer look into the impact of Bernoulli edges on the limit graph structure. As Remark 5.2 pointed out, the sub-critical regime ($a_n^\alpha = n^\gamma \log n$ with $\gamma < 2$) of our toy model could be associated with a motivating example in [4], and so we concentrate on the super-critical regime ($a_n^\alpha = n^\gamma \log n$ with $\gamma > 2$) in this section. For explicitness, as in Section 3, we still take the i.i.d. X_i to have pdf $\alpha x^{-\alpha-1} dx \mathbf{1}_{\{x \geq 1\}}$, i.e. $P(X_i > x) \sim x^{-\alpha}$. However, to take into consideration of both hard edges and Bernoulli edges, the edge connection probability will be $\min\{1, X_i X_j / a_n\}$ rather than $\mathbf{1}_{\{X_i X_j / a_n > 1\}}$.

As before, let $K_{n,0} = \sum_{i=1}^n \mathbf{1}_{\{X_i / \sqrt{a_n} > 1\}}$ denote the number of vertices in the clique. Since the individual vertex statistics stays the same, as in the hard edge only case of Section 3, $K_{n,0} \rightarrow 0$ with probability 1, and given that $K_{n,0} \geq 1$, clique size $K_{n,0} = 1$ is most likely. Nevertheless, in this modified model, edges are more likely to connect. This means that even if $K_{n,0} = 0$, the typical limiting object may not be an empty

graph. To say the least, even if an empty graph is still the dominant feature, given the appearance of a non-trivial graph, one clique vertex and one follower vertex may not be the most ‘economical’ scenario. We explore these directions below, step by step.

Suppose that $K_{n,0} = 0$, i.e. all vertices X_i are follower vertices satisfying $X_i < \sqrt{a_n}$. Pick an arbitrary vertex X_1 . We examine the probability that this particular vertex is non-isolated.

$$\begin{aligned} \mathbb{P}(X_1 \text{ is non-isolated}) &= \int_1^{\sqrt{a_n}} \alpha x_1^{-\alpha-1} dx_1 \left[\left(1 - \frac{1}{a_n^{\alpha/2}}\right)^{n-1} - \left(\int_1^{\sqrt{a_n}} \left(1 - \frac{x_1 x_2}{a_n}\right) \alpha x_2^{-\alpha-1} dx_2\right)^{n-1} \right] \\ &\sim \int_1^{\sqrt{a_n}} \alpha x_1^{-\alpha-1} dx_1 \left[1 - \left(1 - \frac{\alpha}{\alpha-1} \frac{x_1}{a_n}\right)^{n-1} \right] \sim \begin{cases} 1 & \gamma/\alpha < 1, \\ \frac{\alpha^2}{(\alpha-1)^2} \frac{n}{a_n} & \gamma/\alpha \geq 1. \end{cases} \end{aligned} \quad (6.1)$$

Notice that because of the presence of Bernoulli edges, the probability that no edge is formed between vertex X_1 and the rest of the follower vertices X_2, \dots, X_n gets adapted. The first asymptotics above relies on $\alpha > 1$, a reasonable assumption set in [4]. The second asymptotics in addition follows from analyzing the asymptotic ratio of n/a_n , so is essentially dependant on γ/α . As $n/a_n \rightarrow 0$ for $\gamma/\alpha \geq 1$, a sharp transition occurs at $\gamma = \alpha$: An arbitrary vertex X_1 goes from non-isolated to isolated, both with probability 1 in the limit. We state this finding.

Proposition 6.1. Consider the modified toy model with Bernoulli edges at the super-critical regime ($a_n^\alpha = n^\gamma \log n$ with $\gamma > 2$). Pick an arbitrary vertex X_1 . With probability 1 asymptotically X_1 is non-isolated when $\gamma/\alpha < 1$ and isolated when $\gamma/\alpha \geq 1$.

Since X_1 is non-isolated implies the appearance of a non-empty graph, when $\gamma/\alpha < 1$, we obtain a non-empty graph in the limit with probability 1. This is in sharp contrast to the setting where only deterministic edges are present. (See Section 3).

On the contrary, when $\gamma/\alpha \geq 1$, since an empty graph is equivalent to having all vertices isolated, conditioning on $K_{n,0} = 0$, by symmetry and the inclusion-exclusion principle,

$$\mathbb{P}(\text{graph is empty}) = 1 - \mathbb{P}(\exists \text{ a non-isolated vertex}) \geq 1 - n\mathbb{P}(X_1 \text{ is non-isolated}) \sim 1 - \frac{\alpha^2}{(\alpha-1)^2} \frac{n^2}{a_n}, \quad (6.2)$$

where the asymptotics follows from (6.1). We conclude further that with probability 1, the limit graph is empty when $\gamma/\alpha \geq 2$. Even with the presence of Bernoulli edges, this is similar to the setting of Section 3.

Remark 6.2. Set $\gamma/\alpha \geq 2$. Under appropriate conditions, we may compute the limiting probability of an empty graph by brute force and show that it is approaching 1 directly. The calculation is quite cumbersome compared with the crude estimate above, as we need to perform the asymptotics on the exact formula layer by layer. We show one step below but omit the rest of the technical details.

$$\begin{aligned} \mathbb{P}(\text{graph is empty}) &= \int_1^{\sqrt{a_n}} \alpha x_1^{-\alpha-1} dx_1 \int_1^{\sqrt{a_n}} \left(1 - \frac{x_1 x_2}{a_n}\right) \alpha x_2^{-\alpha-1} dx_2 \\ &\quad \dots \int_1^{\sqrt{a_n}} \left(1 - \frac{x_1 x_n}{a_n}\right) \dots \left(1 - \frac{x_{n-1} x_n}{a_n}\right) \alpha x_n^{-\alpha-1} dx_n \\ &\sim \int_1^{\sqrt{a_n}} \alpha x_1^{-\alpha-1} dx_1 \int_1^{\sqrt{a_n}} \left(1 - \frac{x_1 x_2}{a_n}\right) \alpha x_2^{-\alpha-1} dx_2 \\ &\quad \dots \int_1^{\sqrt{a_n}} \left(1 - \frac{x_1 x_{n-1}}{a_n}\right) \dots \left(1 - \frac{x_{n-2} x_{n-1}}{a_n}\right) \left[1 - \frac{\alpha}{\alpha-1} \left(\frac{x_1}{a_n} + \dots + \frac{x_{n-1}}{a_n}\right)\right] \alpha x_{n-1}^{-\alpha-1} dx_{n-1}. \end{aligned} \quad (6.3)$$

As in Section 3, we proceed to explore the structure of the limit graph when there is a lone clique vertex. Again we observe a sharp transition.

Proposition 6.3. Consider the modified toy model with Bernoulli edges at the super-critical regime ($a_n^\alpha = n^\gamma \log n$ with $\gamma > 2$). Given that the graph is non-empty asymptotically and the clique part contains exactly one vertex, typically there is only one follower vertex connected to this clique vertex when $\gamma/\alpha \geq 2$. This dominant feature however no longer holds when $\gamma/\alpha < 2$.

Proof. We start with the probability of a non-isolated lone clique vertex.

$$\begin{aligned} \mathbb{P}(\text{clique vertex} = 1) &= n \int_{\sqrt{a_n}}^{a_n} \alpha x_1^{-\alpha-1} dx_1 \left[\left(1 - \frac{1}{a_n^{\alpha/2}}\right)^{n-1} - \left(\int_1^{\frac{a_n}{x_1}} \left(1 - \frac{x_1 x_2}{a_n}\right) \alpha x_2^{-\alpha-1} dx_2\right)^{n-1} \right] \\ &\quad + n \int_{a_n}^{\infty} \alpha x_1^{-\alpha-1} dx_1 \left(1 - \frac{1}{a_n^{\alpha/2}}\right)^{n-1}. \end{aligned} \quad (6.4)$$

Here we eliminate the situation where $K_{n,0} = 1$, but no edge is formed between the clique vertex X_1 and the follower vertices X_2, \dots, X_n (taking into account the presence of Bernoulli edges). The scalar n indicates that the clique could be centered at any vertex. The second term on the right is of negligible order $n a_n^{-\alpha}$, while the first term, using that $\alpha > 1$, is asymptotically

$$n \int_{\sqrt{a_n}}^{a_n} \alpha x_1^{-\alpha-1} dx_1 \left[1 - \left(1 - \frac{\alpha}{\alpha-1} \frac{x_1}{a_n}\right)^{n-1} \right] \sim \begin{cases} \frac{n}{a_n^{\alpha/2}} & \gamma/\alpha < 2, \\ \frac{\alpha^2}{(\alpha-1)^2} \frac{n^2}{a_n^{(\alpha+1)/2}} & \gamma/\alpha \geq 2. \end{cases} \quad (6.5)$$

Next we study the probability that only one follower vertex is connected to the lone clique vertex. Still denote by $K_{n,1}$ the number of followers.

$$\begin{aligned} \mathbb{P}(\text{clique vertex} = 1, K_{n,1} = 1) &= n(n-1) \int_{\sqrt{a_n}}^{a_n} \alpha x_1^{-\alpha-1} dx_1 \left(\int_1^{\frac{a_n}{x_1}} \frac{x_1 x_2}{a_n} \alpha x_2^{-\alpha-1} dx_2 + \int_{\frac{a_n}{x_1}}^{\sqrt{a_n}} \alpha x_2^{-\alpha-1} dx_2 \right) \\ &\quad \cdot \left(\int_1^{\frac{a_n}{x_1}} \left(1 - \frac{x_1 x_3}{a_n}\right) \alpha x_3^{-\alpha-1} dx_3 \right)^{n-2} \\ &\sim n(n-1) \int_{\sqrt{a_n}}^{a_n} \alpha x_1^{-\alpha-1} dx_1 \left[\frac{\alpha}{\alpha-1} \frac{x_1}{a_n} + \left(\frac{x_1}{a_n}\right)^\alpha \right] \left(1 - \frac{\alpha}{\alpha-1} \frac{x_1}{a_n}\right)^{n-2} \sim \begin{cases} o\left(\frac{n}{a_n^{\alpha/2}}\right) & \gamma/\alpha < 2, \\ \frac{\alpha^2}{(\alpha-1)^2} \frac{n^2}{a_n^{(\alpha+1)/2}} & \gamma/\alpha \geq 2. \end{cases} \end{aligned} \quad (6.6)$$

Here the scalars n and $n-1$ in the equality indicate that the clique could be centered at any vertex and the follower could come from any of the remaining vertices. When $\gamma/\alpha \geq 2$, this probability is asymptotically the same as having a lone clique star graph that was established previously. In contrast, when $\gamma/\alpha < 2$, this probability is asymptotically of lower order than the probability of a lone clique star graph. In fact, we may verify through heavy computation that the probability of any k -star feature by itself is of negligible order as compared with that of a lone clique star graph. We omit the technical details. \square

Propositions 6.1 and 6.3 do not come as a surprise, as the value of a_n (so ultimately γ/α) tunes the number of Bernoulli edges, the larger a_n (γ/α) is, the fewer Bernoulli edges are present. Nonetheless, the abrupt transition instead of a gradual change in the structure of the limiting object is quite an interesting phenomenon.

ACKNOWLEDGEMENTS

Mei Yin's research was supported in part by the University of Denver's Faculty Research Fund. She acknowledges helpful conversations with Yufei Zhao, and is particularly thankful to Yizao Wang for many constructive comments.

REFERENCES

- [1] Arratia, R., Goldstein, L., and Gordon, L. (1989). Two moments suffice for Poisson approximations: The Chen-Stein method. *Ann. Probab.*, 17(1):9–25.
- [2] Borgs, C., Chayes, J. T., Cohn, H., and Holden, N. (2018a). Sparse exchangeable graphs and their limits via graphon processes. *J. Mach. Learn. Res.*, 18(210):1–71.
- [3] Borgs, C., Chayes, J. T., Cohn, H., and Zhao, Y. (2018b). An L^p theory of sparse graph convergence II: LD convergence, quotients, and right convergence. *Ann. Probab.*, 46(1):337–396.

- [4] Borgs, C., Chayes, J. T., Cohn, H., and Zhao, Y. (2019). An L^p theory of sparse graph convergence I: Limits, sparse random graph models, and power law distributions. *Trans. Amer. Math. Soc.*, 372(5):3019–3062.
- [5] Borgs, C., Chayes, J. T., Lovász, L., Sós, V. T., and Vesztergombi, K. (2008). Convergent sequences of dense graphs I: Subgraph frequencies, metric properties and testing. *Adv. Math.*, 219(6):1801–1851.
- [6] Caron, F. and Fox, E. B. (2017). Sparse graphs using exchangeable random measures. *J. R. Stat. Soc. Ser. B. Stat. Methodol.*, 79(5):1295–1366.
- [7] Dabrowski, A. R., Dehling, H. G., Mikosch, T., and Sharipov, O. (2002). Poisson limits for U -statistics. *Stochastic Process. Appl.*, 99(1):137–157.
- [8] Janson, S. (2017). On convergence for graphexes. arXiv:1702.06389.
- [9] Janson, S. (2018). On edge exchangeable random graphs. *J. Stat. Phys.*, 173(3-4):448–484.
- [10] Jessen, A. H. and Mikosch, T. (2006). Regularly varying functions. *Publ. Inst. Math. (Beograd) (N.S.)*, 80(94):171–192.
- [11] Resnick, S. I. (2007). *Heavy-tail Phenomena*. Springer Series in Operations Research and Financial Engineering. Springer, New York. Probabilistic and Statistical Modeling.
- [12] Shorack, G. R. (1972). Functions of order statistics. *Ann. Math. Statist.*, 43(2):412–427.
- [13] Shorack, G. R. (1973). Convergence of reduced empirical and quantile processes with application to functions of order statistics in the non-i.i.d. case. *Ann. Statist.*, 1(1):146–152.

DEPARTMENT OF MATHEMATICS, UNIVERSITY OF DENVER, DENVER, CO 80208
E-mail address: mei.yin@du.edu